Funded by the European Union

UNDINE	
Project number:	101057100
Project name:	The human genetic and immunological determinants of the clinical manifestations of SARS-CoV-2 infection: Towards personalised medicine
Topic:	HORIZON-HLTH-2021-DISEASE-04-07
Type of action:	HORIZON Research and Innovation Actions (RIA)
Starting date of action:	1 June 2022
Project duration:	48 months
Project end date:	31 May 2026
Deliverable number:	D2.5
Deliverable title:	Characterization of impact of entry route and viral variant on cytokine/ISG induction
Document version:	Ver1.0
WP number:	WP2
Lead beneficiary:	IP
Main author(s):	Stefan Pöhlmann (DPZ)
Internal reviewers:	Trine Mogensen (AU)
Nature of deliverable:	R
Dissemination level:	PU
Delivery date from Annex 1:	M48
Actual delivery date:	M48

Funded by the European Union. Views and opinions expressed are however those of the author(s) only and do not necessarily reflect those of the European Union or HADEA. Neither the European Union nor the granting authority can be held responsible for them

Executive Summary

The SARS-CoV-2 spike protein (S) mediates viral entry into host cells and is the main target of the neutralising antibody response. For host cell entry, the S protein binds to the cellular receptor ACE2, followed by proteolytic activation by host cell proteases, with S protein activation by TMPRSS2 being critical for entry into lung cells.

One goal of our project was to determine whether the entry factors discussed above are polymorphic and whether these polymorphisms are associated with functional alterations in the entry process and changes in susceptibility to SARS-CoV-2 infection. Several ACE2 polymorphisms were functionally analysed. However, the impact of these polymorphisms on ACE2 receptor function was modest, and in-depth analysis showed no significant enrichment in resistor cohorts. No candidate polymorphisms were identified in TMPRSS2.

In contrast, polymorphisms in SARS-CoV-2 that discriminate between the closely related variants JN.1 and KP.3.1.1 were found to critically impact lung cell infection. Thus, JN.1 infected primary lung cells in air–liquid interface cultures and precision-cut lung slices with reduced efficiency compared with KP.3.1.1. This phenotype correlated with greater susceptibility of JN.1 infection to MDA5-dependent inhibition and was not observed at temperatures that mimic the upper respiratory tract. These findings suggest that SARS-CoV-2 variants can tolerate increased sensitivity to innate immune inhibition in the lower respiratory tract, as long as efficient replication and spread in the upper respiratory tract are preserved.

Abbreviations

D	Deliverable
EC	European Commission
WP	Work Package
WT	Work Task

Contents

List of Figures

1 Report

1.1 Background

The overall goal of our project is to identify differences in the cellular entry pathways used by SARS-CoV-2 variants and to determine how these differences influence sensitivity to interferon-stimulated genes (ISGs) and modulation of host cell gene expression. One aim is to leverage the expertise and patient data available within UNDINE to determine whether polymorphisms in viral entry factors affect SARS-CoV-2 entry into cultured cells, susceptibility to infection, and disease course. Here, we report the results corresponding to deliverable D2.5: "**List of entry factor polymorphisms that impact susceptibility to infection and course of disease**."

1.2 Results

1.2.1 Impact of ACE2 polymorphisms on viral entry

We and others previously showed that the SARS-CoV-2 spike protein employs the cellular protein ACE2 as a receptor and the cellular serine protease TMPRSS2 as an activator for entry into lung cells (1). An initial analysis identified several ACE2 polymorphisms in a resistor cohort that warranted functional investigation. To this end, ACE2 expression constructs harbouring the respective mutations were generated and verified by sequencing. Expression of the ACE2 variants in transiently transfected BHK-21 cells revealed comparable protein levels in cell lysates, as determined by immunoblotting (**Figure 1A**), and on the cell surface, as determined by fluorescence-activated cell sorting (FACS, **Figure 1B**). Thus, none of the mutations markedly affected ACE2 expression, at least in the context of transient overexpression.

We next analysed whether the mutations affected binding of the viral S protein to ACE2. For this purpose, the S1 subunits of the B.1 and BA.4/BA.5 spike proteins (which are identical at the amino acid level and are therefore collectively referred to as BA.4-5) were fused to the Fc portion of human immunoglobulin. The fusion proteins were expressed in 293T cells, and their binding to ACE2-transfected BHK-21 cells was examined using flow cytometry as the readout. As expected, both the B.1 and BA.4-5 S protein Fc fusion proteins bound efficiently to ACE2-expressing cells but not to control cells, but none of the ACE2 mutations significantly altered binding efficiency (**Figure 1C**).

Finally, we determined whether the mutations affected viral entry into cells. To this end, the ACE2 mutants were transiently expressed in BHK-21 cells, which were subsequently infected with single-cycle vesicular stomatitis virus particles bearing the indicated S proteins and harbouring a reporter genome encoding luciferase. In addition to the S proteins of B.1 and BA.4-5, we included the B.1.617.2, BA.1, XBB.1.5, and XBB.1.16 spike proteins in order to cover a broader range of variants. Quantification of luciferase activity in lysates from infected cells revealed that most ACE2 mutations did not significantly alter the efficiency of viral entry. However, the N720D mutation reduced entry driven by B.1, B.1.617.2, and BA.1 spike proteins, while the L731F mutation reduced entry mediated by B.1 and B.1.617.2 spike proteins (**Figure 1D**).

Since some mutations showed an effect on ACE2 receptor function, the corresponding polymorphisms were analysed in greater depth in patient cohorts. However, no statistically significant associations were observed. Similarly, no polymorphisms in TMPRSS2 were identified that warranted further analysis.

1.2.2 Impact of spike polymorphisms on viral entry and interferon responses

Although the analysis of polymorphisms in the genes encoding for entry factors did not yield notable results, the analysis of polymorphisms characteristic of viral variants, resulted in interesting data. Within UNDINE, we previously discovered that the Omicron subvariant BA.2.86, unlike all previous Omicron subvariants, had regained the capacity to use TMPRSS2 with high efficiency for S protein activation and to enter Calu-3 lung cells with the same efficiency as the virus circulating in Wuhan at the beginning of the pandemic (2). Furthermore, we demonstrated that a single mutation in the S protein of the BA.2.86 derivative JN.1 increased antibody evasion, allowing the virus to become globally dominant (3).

JN.1 infects lung cells less efficiently than KP.3.1.1

We next analysed whether authentic JN.1 and KP.3.1.1 differed in the ability to infect lung cells. We found that infection of primary respiratory epithelial cells cultured at the air liquid interface (ALI) and of precision cut lung slices (PCLS) with authentic KP.3.1.1 was more efficient than that measured for JN.1 (**Figure 2A**), raising the question which mechanisms underlie this difference.

MDA5 knockout results in comparable lung cell infection by KP.3.1.1 and JN.1

We first determined whether the differential lung cell infection by JN.1 and KP.3.1.1 was due to differential lung cell entry but obtained a negative result - the spike proteins of JN.1 and KP.3.1.1 facilitated lung cell entry of pseudotyped single-cycle viral reporter particles with similar efficiency (not shown). Next, we examined whether differential recognition of JN.1 and KP.3.1.1 by sensors and of the IFN system (or, more likely, differential failure to counteract sensing) might be responsible for the differential lung cell infection. Indeed, we found that knock-out (KO) of MDA5 and the adapter protein MAVS resulted in comparable lung cell infection by JN.1 and KP.3.1.1 while this effect was not detected upon RIG-I KO (**Figure 2B**). Further, this effect was specific to the JN.1 variant (**Figure 2C**). Thus, the reduced lung cell infection by JN.1 as compared to KP.3.1.1 was due to increased recognition by MDA5/lack of efficient viral counteraction. In keeping with this concept, lung cell infection by JN.1 resulted in higher induction of IFN and IL-6 as compared to infection by KP.3.1.1 (data not shown).

Similar lung cell infection by JN.1 and KP.3.1.1 at 33°C

We next addressed whether the differential lung cell infection measured for JN.1 and KP.3.1.1 at 37°C would also be observed at 33°C. This temperature is prevalent in the upper respiratory tract and there is evidence that the IFN response at 33°C/in the upper respiratory tract is less potent as compared to 37°C/the lower respiratory tract (4, 5). Interestingly, lung cell infection by JN.1 and KP.3.1.1 was comparable at 33°C (**Figure 2D**), suggesting that increased recognition of JN.1 by MDA5 may be compatible with robust viral spread in the upper respiratory tract and efficient human-human transmission due to reduced potency of the IFN system in this compartment.

2 Conclusion

Within the cohorts analysed, no correlation was observed between polymorphisms in SARS-CoV-2 entry factors and susceptibility to infection. In contrast, we found that the closely related variants JN.1 and KP.3.1.1 differed in their ability to infect lung cells due to differences in their capacity to counteract MDA5, while exhibiting similar infectivity under conditions chosen to mimic the upper respiratory tract. These findings suggest that SARS-CoV-2 evolution may tolerate increased susceptibility to innate immune inhibition in the lower respiratory tract, provided that efficient spread in the upper respiratory tract is maintained.

3 References

1. Hoffmann M, Kleine-Weber H, Schroeder S, Kruger N, Herrler T, Erichsen S, Schiergens TS, Herrler G, Wu NH, Nitsche A, Muller MA, Drosten C, Pohlmann S. 2020. SARS-CoV-2 Cell Entry Depends on ACE2 and TMPRSS2 and Is Blocked by a Clinically Proven Protease Inhibitor. Cell 181:271-280 e8.

2. Zhang L, Kempf A, Nehlmeier I, Cossmann A, Richter A, Bdeir N, Graichen L, Moldenhauer AS, Dopfer-Jablonka A, Stankov MV, Simon-Loriere E, Schulz SR, Jack HM, Cicin-Sain L, Behrens GMN, Drosten C, Hoffmann M, Pohlmann S. 2024. SARS-CoV-2 BA.2.86 enters lung cells and evades neutralizing antibodies with high efficiency. Cell 187:596-608 e17.

3. Zhang L, Dopfer-Jablonka A, Cossmann A, Stankov MV, Graichen L, Moldenhauer AS, Fichter C, Aggarwal A, Turville SG, Behrens GMN, Pohlmann S, Hoffmann M. 2024. Rapid spread of the SARS-CoV-2 JN.1 lineage is associated with increased neutralization evasion. iScience 27:109904.

4. Sposito B, Broggi A, Pandolfi L, Crotta S, Clementi N, Ferrarese R, Sisti S, Criscuolo E, Spreafico R, Long JM, Ambrosi A, Liu E, Frangipane V, Saracino L, Bozzini S, Marongiu L, Facchini FA, Bottazzi A, Fossali T, Colombo R, Clementi M, Tagliabue E, Chou J, Pontiroli AE, Meloni F, Wack A, Mancini N, Zanoni I. 2021. The interferon landscape along the respiratory tract impacts the severity of COVID-19. Cell 184:4953-4968 e16.

5. V'Kovski P, Gultom M, Kelly JN, Steiner S, Russeil J, Mangeat B, Cora E, Pezoldt J, Holwerda M, Kratzel A, Laloli L, Wider M, Portmann J, Tran T, Ebert N, Stalder H, Hartmann R, Gardeux V, Alpern D, Deplancke B, Thiel V, Dijkman R. 2021. Disparate temperature-dependent virus-host dynamics for SARS-CoV-2 and SARS-CoV in the human respiratory epithelium. PLoS Biol 19:e3001158.

Figure 1

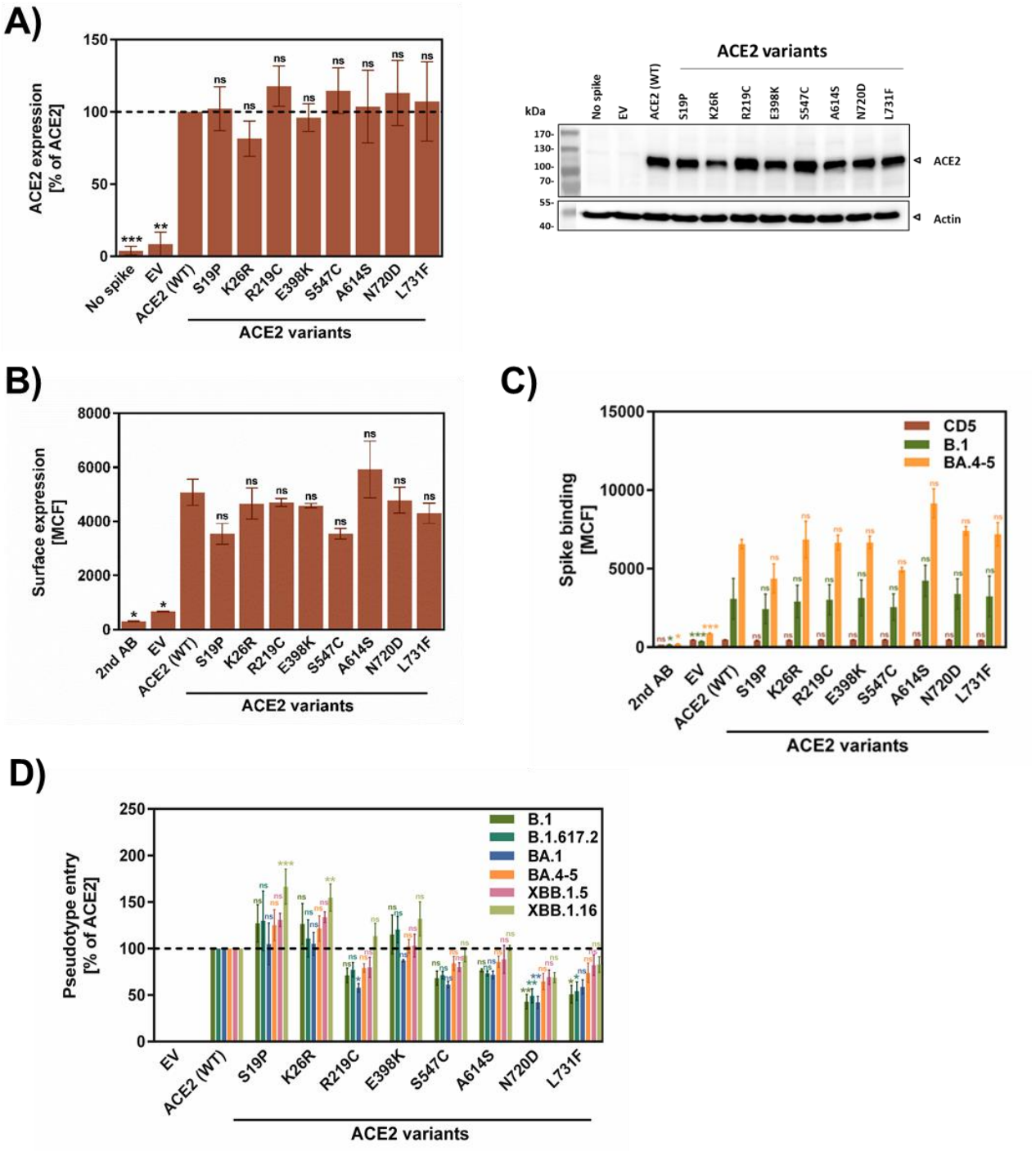

Figure 1: Impact of ACE2 polymorphisms on receptor function.

(A) BHK-21 cells were transfected with plasmids encoding the indicated ACE2 mutants corresponding to polymorphisms identified in patients. ACE2 expression was analysed by immunoblotting. Signals were quantified, and the average of three independent experiments is shown in the left panel, while a representative blot is shown in the right panel.

(B) The experiment was carried out as described for panel A, but ACE2 surface expression was quantified by flow cytometry.

(C) The indicated ACE2 variants were transiently expressed in 293T cells, which were subsequently incubated either with the Fc portion of human immunoglobulin (containing the signal peptide of CD5, CD5-Fc) or with the S1 subunit of B.1 or BA.4/5 spike fused to Fc. Binding efficiency was then determined by flow cytometry.

(D) The experiment was carried out as described for panel C, except that the cells were infected with pseudoparticles bearing the indicated spike proteins. Luciferase activity in cell lysates was determined 16 h post infection. Panels B–D show the average ± SEM of three independent experiments.

Figure 2

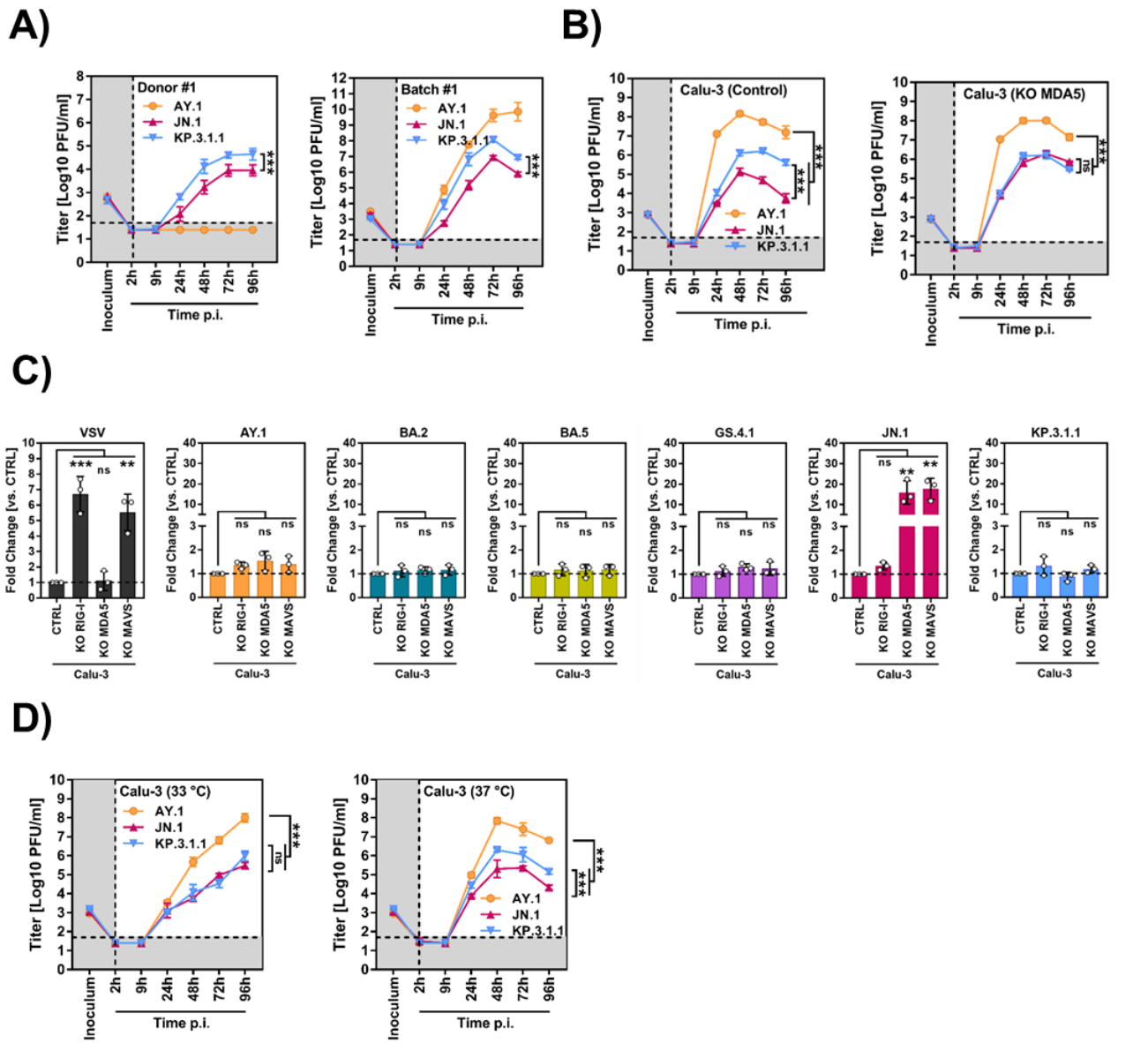

Figure 2: Evidence that JN.1 has a reduced capacity to counteract detection by MDA5

(A) Precision-cut lung slices (PCLS, kindly provided by Prof. Armin Braun, Fraunhofer ITEM, Hannover, Germany; left panel) or primary human airway epithelial cells cultivated at the air-liquid interface (kindly provided by Prof. Martin Ulrich, Hannover Medical School, Hannover, Germany; right panel) were infected with the indicated viruses and production of progeny virions over time quantified by plaque assay. The results of a single representative experiment carried out with triplicate samples are shown and were confirmed with cells from two-three different donors/batches.

(B) The experiment was carried out as described for panel A but Calu-3 WT cells or Calu-3 cells lacking MDA5 (kindly provided by Caroline Goujon, IRIM, CNRS, Montpellier University, Montpellier, France) were infected. Data represent the average (mean) of three independent experiments. Error bars indicate the SEM.

(**C**) The experiment was carried out as described for panel A but the indicated Calu-3 cell lines and SARS-CoV-2 variants were used for infection and augmentation of infection relative to WT cells is

indicated at 48 h post infection. Data represent the average (mean) of three independent experiments. Error bars indicate the SEM.

(**D**) The experiment was carried out as described for panel A but Calu-3 WT cells were infected at 33°C and 37°C. Data represent the average (mean) of three independent experiments. Error bars indicate the SEM.